Heliyon 9 (2023) e20028

Contents lists available at ScienceDirect

Heliyon

journal homepage: www.cell.com/heliyon

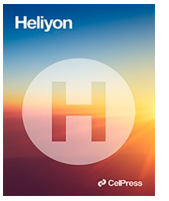

Cellular uptake, intracellular behavior, and acute/sub-acute cytotoxicity of a PEG-modified quantum dot with promising *in-vivo* biomedical applications

Qingyuan Cheng [a,b,1], Yiping Duan [c,1], Wei Fan [d,1], Dongxu Li [a], Cuiwen Zhu [a], Tiantian Ma [a], Jie Liu [e,**], Mingxia Yu [a,*]

[a] Department of Laboratory Medicine, Zhongnan Hospital of Wuhan University, Wuhan, Hubei, China
[b] Department of Andrology/Sichuan Human Sperm Bank, West China Second University Hospital, Sichuan University, Chengdu, Sichuan, China
[c] Department of Laboratory Medicine, the Third Hospital of Wuhan, Wuhan, Hubei, China
[d] Department of Pathology, Zhongnan Hospital of Wuhan University, Wuhan, Hubei, China
[e] Department of Endocrinology, Zhongnan Hospital of Wuhan University, Wuhan, Hubei, China

ARTICLE INFO

Keywords:
Quantum dots
Polyethylene glycol modification
Cellular uptake
Intracellular behavior
Sub-acute cytotoxicity

ABSTRACT

Quantum Dots (QDs) modified with branched Polyethylene Glycol-amine (6- or 8-arm PEG-amine) coupled with methoxy PEG (mPEG) hold great promise for *in vivo* biomedical applications due to a long half-life in blood and negligible toxicity. However, the potential risks regarding their concomitant prolonged co-incubation with cardiovascular and blood cells remains inconclusive. In the present study, the feasible, effective and convenient proliferating-restricted cell line models representing the circulatory system were established to investigate the cellular internalization followed by intracellular outcomes and resulting acute/sub-acute cytotoxicity of the 6-arm PEG-amine/mPEG QDs. We found a dose-, time- and cell type-dependent cellular uptake of the 6-arm PEG-amine/mPEG QDs, which was ten-fold lower compared to the traditional linear PEG-modified counterpart. The QDs entered cells via multiple endocytic pathways and were mostly preserved in Golgi apparatus for at least one week instead of degradation in lysosomes, resulting in a minimal acute cytotoxicity, which is much lower than other types of PEG-modified QDs previously reported. However, a sub-acute cytotoxicity of QDs were observed several days post exposure using the concentrations eliciting no-significant acute cytotoxic effects, which was associated with elevated ROS generation caused by QDs remained inside cells. Finally, a non-cytotoxic concentration of the QDs was identified at the sub-acute cytotoxic level. Our study provided important information for clinical translation of branched PEG-amine/mPEG QDs by elucidating the QDs-cell interactions and toxicity mechanism using the proliferation-restricted cell models representing circulatory system. What's more, we emphasized the indispensability of sub-acute cytotoxic effects in the whole biosafety evaluation process of nanomaterials like QDs.

* Corresponding author.
** Corresponding author.
E-mail addresses: zn000752@whu.edu.cn (J. Liu), dewrosy520@whu.edu.cn (M. Yu).
[1] Qingyuan Cheng, Yiping Duan and Wei Fan contributed equally to this work.

https://doi.org/10.1016/j.heliyon.2023.e20028
Received 26 April 2023; Received in revised form 21 August 2023; Accepted 8 September 2023
Available online 9 September 2023

1. Introduction

Quantum dots (QDs) are semiconductor nanocrystals that exert excellent optical properties, high stability, and biocompatibility after appropriate surface modifications. QDs have promising biomedical applications, such as live-cell labeling and *in vivo* imaging in clinic [1,2]. Despite many encouraging results, the concerns on non-specific binding of QDs and potential bio-safety issues have hindered their clinical translation [3]. It is generally accepted that the non-specific binding and cytotoxic effects of QDs are a cumulative function of QDs composition and structure, surface properties, exposure dose and time as well as cell types [4,5]. Among these factors, the surface properties of QDs are the most important because it not only determines the strength of QDs-cells interactions but also has a great impact on the endocytosis of QDs that is the main uptake mechanism of QDs by cells. Fortunately, the latter can be controlled by coating QDs with ligands [6,7]. Different ligands on the surface of QDs trigger different endocytic pathways and entry of QDs into different intracellular regions, leading to different cytotoxic effects [8–12]. Therefore, optimal modification of surface is an effective way to minimize non-specific binding and cytotoxicity of QDs [13].

Surface modification of QDs with polyethylene glycol (PEG) is a main strategy to extend and improve the *in vivo* biomedical applications of QDs by significantly decreasing the non-specific binding and cytotoxicity of QDs via its ability to inhibit the QDs-cells interaction and cellular uptake. The endocytosis and subcellular localization of QDs could be further modulated through using PEGs with different molecular weights, structures, and terminal functional groups, which allows the more flexibility for attaining optimized biocompatibility of QDs [14,15]. In recent years, the near-infrared fluorescent QDs coated with the branched PEG (6-arm or 8-arm) with terminal amino groups and the PEG with terminal methoxy groups (branched PEG-amine/mPEG QDs) were reported to have minimal non-specific binding effect, the longest blood-circulation half-life (at 7 h), and negligible toxic effects [16,17]. Thus, this type of PEG modification is suitable for *in vivo* biomedical imaging applications, such as real-time tumor detection to guide surgical operation [18,19]. There were many studies reporting the biodistribution of near-infrared QDs with similar PEG-modifications. Most of QDs were accumulated in the liver and spleen and the majority of QDs inside the body were eliminated though feces [16,20]. Despite distinct advantages of branched PEG-amine/mPEG QDs established by multiple studies, the underlying mechanisms of cellular uptake, intracellular life cycle, and cytotoxic effects of it have not been explored to date. Such mechanism are expected to differ from other PEG-modified QDs and needed to be clearly elucidated, which is vital for facilitating successful clinical translation of such surface engineered QDs.

The branched PEG-amine/mPEG QDs was previously found to exhibit a slightly deleterious effect under scenarios rather different from the *in vivo* clinical application. These cytotoxicity assays were usually performed on cancer cell lines. However, since intravenous injection is the most common way of delivering those fluorescent probes into body, cells representing the circulatory system are more suitable *in vitro* models than solid tumor cells for assessing toxicity of QDs [21,22]. Additionally, these studies only assessed acute-cytotoxic (no more than 24 h), which may miss sub-acute cytotoxicity observable after a longer time [23]. The sub-acute cytotoxicity is of particular relevance to clinical translation of branched PEG-amine/mPEG QDs because intravenous administration of them results in a prolonged co-existence with cells in the circulatory system, which may cause elevated risks of blood and vessel damage [24]. Hence, the *in vitro* toxicity assessment of branched PEG-amine/mPEG QDs so far is inadequate. In the context of *in vivo* bio-medical applications via intravenous administration, there is the need for more rigorous evaluation of cardiovascular and blood safety issues caused by branched PEG-amine/mPEG QDs during prolonged circulation process. This work was designed to provide new insights into the safety of branched PEG-amine/mPEG QDs to pave the way for its safe clinical translation.

2. Experimental section

2.1. Chemicals and materials

The oleic acid capped ZnCdSe@ZnS QDs (Product Code: Q1625) and PEG-amine QDs (Product Code: Q4625, MW of PEG-amine = 2 K, linear chain) were purchased from Wuhan Jiayuan Quantum Dots Co., Ltd (Wuhan, Hubei, China). 1-Ethyl-3-[3- dimethylaminopropyl] carbodiimide (EDC) was purchased from Thermo Fisher Scientific Inc. (Waltham, MA, USA). 6-arm PEG-amine (molecular mass ≈ 10 K) and mPEG-amine (molecular mass ≈ 1 K) were purchased from Shanghai Ponsure Biotechnology (Shanghai, China). Phorbol-12-myristate-13-acetate (PMA), methyl-β-cyclodextrin (MβCD) and chlorpromazine (CPM) were purchased from Aladdin (Shanghai, China). All of the chemicals were used as received without further purification.

2.2. Preparation and characterization of 6-arm PEG-amine/mPEG QDs

Because that near-infrared QDs were inconvenient in *in vitro* imaging, in the present study, the classical ZnCdSe/ZnS core-shell QDs was selected and modified with 6-arm PEG-amine/mPEG, as an appropriate substitute for near-infrared QDs to investigate the cellular uptake and intracellular behavior of branched PEG-amine/mPEG QDs easier. Notably, ZnCdSe/ZnS core-shell QDs was merely used as a model, it will not be applied in the biomedicine. Hydrophilic QDs were prepared by coating with the amphiphilic polymer, octylamine-modified polyacrylic acid (OPA), which were then dispersed in borate saline buffer (0.05 M, pH = 7.0) according to previous reports [25,26]. This material is designated as OPA-QDs. For further PEG modification, 10 mg of 6-arm PEG-amine, 20 mg of mPEG-amine, and 10 mg of EDC were added into the 4 mL of OPA-QDs (10 nM) for conjugation. The mixture was allowed to react for 3 h at 37 °C under continuous agitation and then purified by centrifugal filter devices (Millipore Amicon, Ultra-15/100 kDa, Millipore, MA, USA) with borate saline buffer (0.05 M, pH = 8.4) for 3 times. In the final step, the PEG-amine QDs (8 μM) and 6-arm PEG-amine/mPEG QDs (5 μM) was dispersed in 1 × PBS buffer, sterilized by passing through a 0.22 μm microfilter (Millipore, MA,

USA) and then stored at 4 °C.

The shape and size of the 6-arm PEG-amine/mPEG QDs were characterized by transmission electron microscope (TEM) (JEM-2010FEF (UHR), JEOL, Tokyo, Japan), operated at 200 kV. The absorption and fluorescence spectra of 6-arm PEG-amine/mPEG QDs were measured by an ultraviolet–visible spectrophotometer (UV2550, Shimadzu, Kyoto, Japan) and a fluorescence spectrophotometer (Fluorolog-3, Horiba Jobin Yvon, Paris, France). The hydrodynamic diameter and zeta potential of the as-prepared samples were determined by dynamic light scattering (DLS) (Zetasizer Nano ZS, Malvern Instruments, Malvern, UK) at room temperature. Agarose gel electrophoresis of 6-arm PEG-amine/mPEG QDs was performed using 1% (w/v) Tris-acetic acid-ethylenediaminetetraacetic acid (TAE) buffer, and images was captured using a gel imaging system under UV light (Tanon-5200, Shanghai, China).

2.3. Cell culture, establishment and verification of proliferation-restricted cells

Two representative circulatory system cell lines, human monocytic leukemia cell line THP-1 and human umbilical vein endothelial cells (HUVEC), were chosen and induced to proliferation-restricted cell models inspired by Soenen. et al. [23,27–29]. Such simple cell models are effective and robust for evaluating acute and subacute toxicity of nanomaterials. In *in vitro* cell lines, intracellular QDs were diluted quickly due to the cell division, which was different from cells in *in vivo* environment. The use of proliferation-restricted cell models could avoid this and thus better simulate the real situation *in vivo* [30]. The prepared QDs were co-cultured with these proliferation-restricted cells to investigate their cellular uptake, intracellular distribution and the consequential cytotoxic effects. The acute cytotoxicity of QDs were assessed after 24 h and sub-acute cytotoxicity was assessed after 7 days of exposure to QDs for 24 h at a concentration without acute cytotoxicity. Several *in vitro* assays were subsequently conducted, in combination with known intracellular behaviors of QDs, to understand cytotoxic mechanisms of the QDs on circulatory system cells.

Human monocytic leukemia cell line THP-1 were obtained from ATCC (ATCC Cell lines Service, MA, USA). Cells were cultured in RPMI-1640 medium (Hyclone, GE Healthcare, Boston, MA, USA), supplemented with 10% fetal bovine serum and 1% penicillin/streptomycin (Gibco, Invitrogen, Waltham, MA, USA). To establish proliferation-restricted cell cultures, THP-1 cells were differentiated into macrophage cells (THP-1 MΦ) by treating with fresh media containing PMA (5 ng/mL). Most cells were attached after 24 h. Then the PMA-containing medium was replaced by the fresh normal medium. THP-1 MΦ cells ceased to proliferate and were in good shape for weeks.

Human umbilical vein endothelial cells, HUVEC, was purchased from ATCC (ATCC Cell lines Service, MA, USA). Cells was maintained in DMEM (Hyclone, GE Healthcare, Boston, MA, USA) containing 10% fetal bovine serum and 1% penicillin/streptomycin (Gibco, Invitrogen, Waltham, MA, USA). To establish proliferation-restricted cell populations, HUVEC cells were given culture medium with a lower concentration serum (1%) when the confluence of cells reached 80%. Cell proliferation was then minimized, and confluent cells were maintained under this culture conditions for at least one week.

To verify the successful establishment of proliferation-restricted cells of THP-1 and HUVEC, cell proliferation activity was determined using 5-ethynyl-20-deoxyuridine (EdU) kit (BeyoClick™ EdU Cell Proliferation Kit with Alex Fluor 488, Beyotime, Shanghai, China) as per manufacturer's instructions. Briefly, the THP-1 MΦ and non-proliferating HUVEC cells were seeded in 24-well plates with cell climbing slice. THP-1 and HUVEC cells were used as control. After culturing for 2 or 3 days, cells were incubated with culture medium containing 10 μM EdU for 2 h, washed and fixed with 4% paraformaldehyde for 15 min, and permeated with 0.3% Triton X-100 for another 15 min. Cells were stained with the Click Reaction Mixture for 30 min at room temperature and Hoechst 33342 for another 10 min. The cells were observed and photographed with a fluorescence microscope (BX53, Olympus, Tokyo, Japan), where cells undergoing rapid proliferation exhibit bright green fluoresce color.

For further assessing the inhibition of cell cycle progression, cell cycle phase distribution in THP-1, THP-1 MΦ, HUVEC and non-proliferating HUVEC cells was detected with Propidium iodide (PI) staining (Cell Cycle Staining Kit, MultiSciences, Hangzhou, Zhejiang, China) according to the manufacturer's protocol. Briefly, cells were harvested, washed and then treated with RNase A and PI at room temperature in the dark for 30 min. Cells were analyzed via a flow cytometry (Cytoflex, Beckman, CA, USA) and at least 10000 cells were counted.

2.4. Endocytosis pathway analysis and intracellular imaging of QDs

For quantitative measurement of QDs cellular uptake, THP-1 MΦ and non-proliferating HUVEC cells were incubated with culture media containing different concentrations of OPA-QDs, PEG-amine QDs, and 6-arm PEG-amine/mPEG QDs in 6-well plates for 1, 6 and 24 h. Then, cells were washed and analyzed by flow cytometry. For endocytic pathway inhibition study, THP-1 MΦ and non-proliferating HUVEC cells were pretreated with culture media containing MβCD (1 mM) or CPM (10 μM) at 37 °C for 30 min. Then, cells were washed with a PBS buffer after inhibitor-containing medium was removed. After that, cells were incubated with culture media containing 6-arm PEG-amine/mPEG QDs (500 nM) at 37 °C for another 6 h. Subsequently, cells were harvested in vials and washed with PBS buffer for three times to remove unbound QDs. The amount of QDs endocytosed by cells (defined as the percentage of QDs-positive cells) were determined.

For intracellular imaging of 6-arm PEG-amine/mPEG QDs, above cells were seeded in 24-well plates with cell climbing slice and were induced into proliferation-restricted cells. Next, they were incubated in medium containing 6-arm PEG-amine/mPEG QDs (250 nM for THP-1 MΦ and 500 nM for non-proliferating HUVEC) at 37 °C for 6 h. After that, cells were washed with PBS buffer and stained with Hoechst 33342. To observe spatiotemporal distribution of 6-arm PEG-amine/mPEG QDs at the subcellular level, cells were washed with PBS buffer for three times to remove the unbound QDs and were maintained with proliferation-restricted condition till the different time points after incubation (1, 6, 24, 48, 72, 120 and 168 h). Then, for cells ready to be imaged, lysosomes were stained using

Lysosensor blue DND-167 and Golgi apparatus were stained with NBD C6-ceramide (Invitrogen Molecular Probes, ThermoFisher Scientific, Waltham, MA, USA) according to the manufacturer's protocols. Briefly, the medium was removed, and cells were washed with HBSS buffer for three times. Then, cells were incubated with NBD C6-ceramide to stain Golgi apparatus at 4 °C for 30 min before being washed with cold fresh medium. Subsequently, cells were incubated with Lysosensor blue DND-167 to stain lysosome at 37 °C for another 30 min and washed with fresh medium. Finally, cells were visualized and photographed by a fluorescent microscope (BX53, Olympus, Tokyo, Japan).

2.5. Acute, sub-acute cytotoxicity assays and determination of inhibitory concentration of QDs

For acute cytotoxicity study, viability of THP-1 MΦ and non-proliferating HUVEC cells after exposure to 6-arm PEG-amine/mPEG QDs were determined using cell counting kit-8 (CCK-8) as per manufacturer's instructions (Dojindo, Tokyo, Japan). Briefly, THP-1 and HUVEC cells were seeded in the 96-well plate and were established with proliferation-restricted cell cultures as mentioned above. Then, the cells were incubated with the culture media containing different doses of QDs for 24 h. After that, the cells were washed with PBS buffer, incubated with culture media containing 10% (v/v) CCK-8 solution at 37 °C for 2 h. The absorbance (450 nm) of each well was subsequently measured using a multiplate reader (PE Enspire, PerkinElmer, MA, USA). The 50% and 5% inhibitory concentrations (*IC50* and *IC5*) of each cell line were calculated based on the cell viability data.

For sub-acute cytotoxicity study, cell viability of two proliferation-restricted cells were determined with Alamar Blue assay (Molecular Probes, Invitrogen, Waltham, MA, USA) according to the manufacture's protocol. Briefly, THP-1 and HUVEC cells were seeded in the black 96-well plate and were established with proliferation-restricted cell cultures using the procedure mentioned above. Then, cells were incubated with the culture media containing *IC5* doses of QDs for 24 h. After that, the QDs-containing culture media were removed, and the cells were maintained with medium under proliferation-restricted conditions, containing alamar blue reagent (10% (v/v) for THP-1 MΦ and 5% (v/v) for non-proliferating HUVEC), for one week. Then, fluorescence intensities (λ ex = 545, λ es = 590 nm) of each well were measured using a multiplate reader (PE Enspire, PerkinElmer, MA, USA) after 1, 3, 5 and 7 days of further culture.

2.6. Macrophages IL-6 release assay

THP-1 MΦ cells were incubated with the culture media containing different doses of 6-arm PEG-amine/mPEG QDs for 24 h. The supernatants were recovered and released IL-6 was analyzed using an ELISA kit (Cusabio, Wuhan, Hubei, China) as per manufacturer's instructions.

2.7. Measurement of intracellular ROS formation, mitochondrial membrane potential (MMP) and Lysosomal Membrane Permeabilization (LMP) Analysis

The intracellular ROS formation, the mitochondrial membrane potential (MMP) and lysosomal membrane permeability (LMP) of THP-1 MΦ and non-proliferating HUVEC cells after exposure to 6-arm PEG-amine/mPEG QDs were detected via DCFH-DA (ROS Assay Kit, Beyotime, Shanghai, China), JC-1 kit (Beyotime, Shanghai, China), and Acridine Orange (AO) (Molecular Probes, Invitrogen, Waltham, MA, USA) according to manufacturer's protocol, respectively. For acute study, THP-1 MΦ and non-proliferating HUVEC cells were cultured in 6-well plate, treated with medium containing different concentrations of 6-arm PEG-amine/mPEG QDs at 37 °C for 24 h and then washed three times with PBS buffer to remove unbound QDs. For ROS detection, cells were incubated with medium containing 10 μM DCFH-DA for 30 min. For a positive control, cells were firstly treated with Rosup for 30 min at 37 °C prior to being incubated with 10 μM DCFH-DA-containing medium. For MMP detection, cells were harvested in vials, and the JC-1 was loaded into cells at 37 °C for 20 min. CCCP (10 μM) was used as a positive control. For LMP detection, cells were stained with AO-containing PBS buffer for 15 min(5 μg/mL). After treatment, the cells were washed with PBS buffer for 3 times and observed using a flow cytometer (Cytoflex, Beckman, CA, USA) and at least 10000 cells were counted. For sub-acute study, cells were incubated with a culture medium containing IC5 doses of QDs for 24 h. After that, the QDs-containing culture media were removed, and the cells were continually maintained with medium under proliferation-inhibited conditions and the ROS levels, MMP and LMP of cells were observed and recorded using a fluorescent microscope (Olympus, IX73, Tokyo, Japan) after 1, 3 and 7 days. Only the green fluorescence representing the JC-1 monomers were recorded since the signals of JC-1 aggregates and QDs overlapped at the detection channel of the flow cytometer and the fluorescence microscope. Similar to the measurement of MMP, the red fluorescence representing the protonated oligomeric form of AO cannot be measured due to the fluorescence overlapped with QDs.

2.8. Statistics

Experimental data were processed and analyzed in Flow Jo (V10.0), GraphPad Prism (V8.3.0), Image J (1.53a), Adobe Photoshop and Adobe Illustrator (CC 2017). Unless stated otherwise, results from 3 independent experiments (expressed as mean ± SD) were analyzed via one-way analysis of variance (ANOVA). The Dunnett post-hoc analysis method was conducted to compare experimental groups to the control group. In all cases, to compare experimental/positive groups with the blank group, the level of significance was indicated as, * ($p < 0.05$) and ** ($p < 0.01$). Moreover, to compare the results among different experimental groups, the level of significance was noted as $^{\#}$ ($p < 0.05$) and $^{\#\#}$ ($p < 0.01$).

3. Results

3.1. Characterization of 6-arm PEG-amine/mPEG QDs

Physicochemical properties of 6-arm PEG-amine/mPEG QDs are summarized in Figure S1. The 6-arm PEG-amine/mPEG QDs were monodispersed in the buffer and highly uniform with a core size of approximately 5.4 nm from TEM images (Figure S1A and B). The fluorescence spectrum of the 6-arm PEG-amine/mPEG QDs had a narrow emission with the maximum emission wavelength at 623 nm and a full width at half maximum of 34 nm, same as the original organic phase QDs (Figure S1C). Compared with OPA-QDs, the hydrodynamic size of the 6-arm PEG-amine/mPEG QDs increased from 10.1 nm to 15.7 nm (Figure S1D and E), which was larger than PEG-amine QDs (13 nm) modified with linear chain PEG (molecular mass = 2 K) and was smaller than previously reported QDs coated with 8-arm PEG-amine/mPEG (18.2 nm) [16,26]. For the surface charge, functionalization of OPA-QDs with 6-arm PEG-amine/mPEG shifted zeta potential from −47.6 mV to −7.4 mV, which is much less negatively charged than that functionalized with linear chain PEG-amine (−31 mV) [26]. Moreover, the results of agarose gel electrophoresis showed minimal migration in QDs functionalized with 6-arm PEG-amine/mPEG, suggesting a zwitterionic nature. This can be attributed to the presence of negatively charged carboxyl group of the OPA-QDs and positively charged amino group at the end of PEG (Figure S1F).

3.2. Successful establishment of proliferation-restricted cell cultures

To verify the establishment of proliferation-restricted cell cultures, the cell proliferation activity was detected by EdU assay coupled with cell cycle analysis. As shown in Figure S2, compared with cells cultured in normal condition, the green fluorescence nearly disappeared after non-proliferating treatment, demonstrating the significant inhibition of cell proliferation. Consistent with the results of EdU assay, cell cycle was clearly arrested after treatment, in which cell abundance in S and G2 phase was significant diminished, and more than 90% cells stayed in G1 phase. However, the cell death of THP-1 MΦ and non-proliferating HUVEC cells were not observed after 8 days (Figure S3). Thereby, both proliferation-restricted cell cultures can be used for *in vitro* investigation of the impact of QDs on the intracellular behavior and sub-acute cytotoxicity for at least one week.

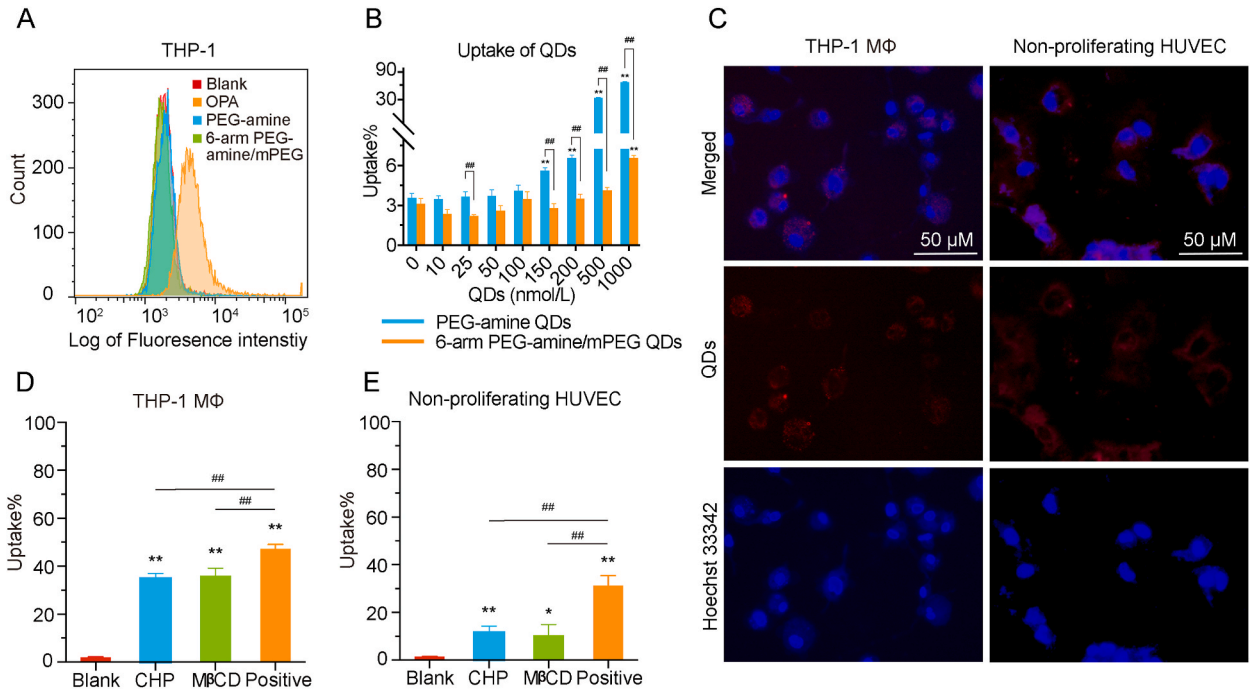

Fig. 1. Cellular uptake of QDs and intracellular imaging of 6-arm PEG-amine/mPEG QDs. (A) THP-1 cells were incubated with OPA-QDs and PEG-modified QDs at the same concentration (100 nM) for 1 h, respectively, then cells were washed and analyzed by flow cytometry. Cellular uptake of PEG-modified QDs were significantly inhibited in comparison to that of OPA-QDs. **(B)** THP-1 cells were incubated with PEG-amine and 6-arm PEG-amine/mPEG QDs at concentrations from 0 nM to 1000 nM for 1 h, respectively. The results clearly indicated a dose-dependent internalization of PEG-modified QDs and a nearly tenfold lower uptake of 6-arm PEG-amine/mPEG QDs compared to PEG-amine QDs. **(C)** THP-1 MΦ cells and non-proliferating HUVEC cells were exposed to QDs (250 nM and 500 nM, respectively) for 6 h, then the cells were washed, stained with Hoechst 33342 and visualized under microscope. The results of intracellular imaging suggested a difference in cellular internalization and subcellular trafficking between two cell models. **(D and E)** THP-1 MΦ cells and non-proliferating HUVEC cells were pretreated with different endocytosis inhibitors for 30 min. Then, cells were washed, incubated with 6-arm PEG-amine/mPEG QDs (500 nM) for another 6 h and determined by flow cytometry. It was observed that both of endocytic pathways were involved in endocytosis of 6-arm PEG-amine/mPEG QDs.

3.3. Effects of exposure time, concentration, and cell type on cellular uptake of 6-arm PEG-amine/mPEG QDs

After incubation with 100 nM of different QDs for 1 h, the QDs-positive cells are approximately 70% for OPA-QDs but are marginal in both PEG-modified QDs, indicating the ability of PEG to suppress the cellular uptake (Fig. 1A). Following 1-h incubation, the cellular internalization is not pronounced until the concentration of PEG-amine QDs reached 200 nM, where QDs-positive cells increased to 68% at 1000 nM (Fig. 1B). However, QDs-positive cells after incubation with 1000 nM 6-arm PEG-amine/mPEG QDs was only about 7%, i.e., about 10% of the case with PEG-amine QDs. The number of cells internalizing 6-arm PEG-amine/mPEG QDs increased remarkably after an extended period of incubation at 500 nM and 1000 nM (Figure S4A and B). At 500 nM, QDs-positive cells after incubation for 6 h and 24 h are 30% and 60%, respectively. However, the percentage of QDs-positive cells at 1000 nM was only slightly higher than that of 500 nM at both time points, hinting at a saturated uptake of QDs (Figure S4C). The time period and concentration of 6-arm PEG-amine/mPEG QDs to reach saturation is far more than those of PEG-amine QDs [31]. After incubating with 500 nM QDs for 6 h, the cellular internalization of 6-arm PEG-amine/mPEG QDs by THP-1 MΦ cells (48.3%) was approximately two times that of non-proliferating HUVEC cells (23.7%), clearly reflecting the different cellular uptake capacity between the two cell types (Figure S4D and E). Intracellular imaging of 6-arm PEG-amine/mPEG QDs also revealed differences between the two cell types (Fig. 1C), where QDs inside THP-1 MΦ cells were encapsulated in spherical vesicles but not in the non-proliferating HUVEC cells.

3.4. Role of clathrin-mediated and lipid raft-mediated pathways in endocytosis of QDs

It is generally accepted that cellular entry and subcellular trafficking of QDs mainly rely on endocytosis [29]. Hence, the difference in uptake amount and intracellular distribution of 6-arm PEG-amine/mPEG QDs between two cell models revealed in previous sections may have originated from different endocytic pathways. Since clathrin-mediated and lipid raft-mediated pathway, both belong to micropinocytosis, play a crucial role in the entry of QDs into cells [32], we explored the potential endocytic pathways of 6-arm PEG-amine/mPEG QDs by using endocytosis inhibitors, CPM for blocking clathrin-mediated and MβCD for blocking lipid raft-mediated endocytosis. Incubation with either inhibitor blocked the cellular uptake of QDs in both cell models (Fig. 1D and E), implying that both of pathways were involved in the endocytosis of the QDs. While the blocking effects of both inhibitors on the entry of QDs into non-proliferating HUVEC cells were significant (70% by MβCD and 60% by CPM), the effects on THP-1 MΦ cells were much milder, with a decrease of the cellular uptake from 48% to 35%. This indicates that other pathways were also involved in the cellular uptake process. MβCD was previously found to efficiently inhibit the entry of PEG-modified QDs with either amino or methoxy terminal functional groups into THP-1 MΦ cells [33]. The different observations may be attributed to the low dosage of QDs applied (2 nM) in the previous study, where the percentages of QDs-positive THP-1 MΦ cells were low in control groups without inhibitors (<15% for PEG-amino QDs and <5% for mPEG QDs).

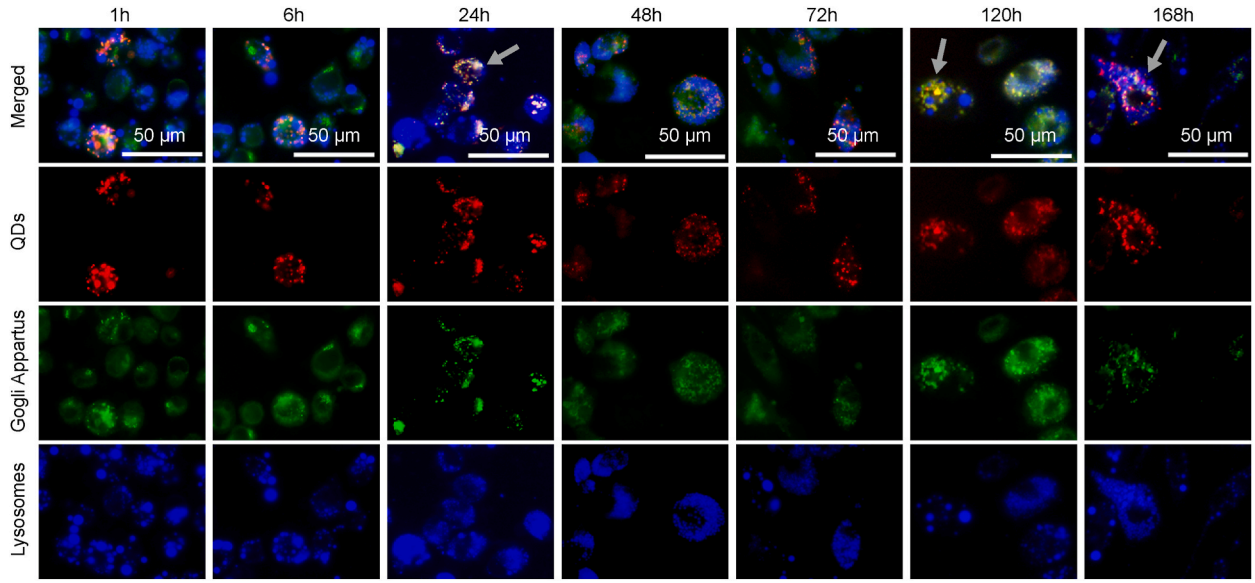

Fig. 2. Representative fluorescence images of spatiotemporal intracellular distribution of 6-arm PEG-amine/mPEG QDs in THP-1 MΦ cells. THP-1 MΦ cells were exposed to QDs (250 nM) for 6 h, then the QDs were removed, and cells were kept cultured for different time points (1, 6, 24, 48, 72, 120 and 168 h). Once above given time points achieved, cells loaded with QDs (red) were stained with fluorescent dye labeling Golgi apparatus (green) and lysosome (blue) for 30 min, respectively, and were imaged under fluorescent microscope. It is clear that QDs inside cells were predominantly localized at Golgi apparatus for at least 168 h after endocytosis (merged images). Some typical colocalizations were noted by grey arrows.

3.5. Subcellular colocalization of 6-arm PEG-amine/mPEG QDs one-week after uptake

The results of the endocytosis inhibition experiment revealed that both clathrin-mediated and lipid raft-mediated pathways participated in cellular uptake of 6-arm PEG-amine/mPEG QDs. It is well known that these two pathways transported QDs to different subcellular regions. Therefore, we further performed the subcellular co-localization analysis in each proliferation-restricted cell model to observe the fate of intracellular QDs one-week after uptake. In the THP-1 MΦ cells (Fig. 2), the bright red fluorescence emitted by QDs overlapped with the green fluorescence emitted by dyes tracking Golgi apparatus from immediately after incubation (1 h) to about 7 days (168 h) (grey arrows). For proliferation-restricted HUVEC cells (Fig. 3), the fluorescence of the QDs was initially co-localized with that of dyes labeling Golgi apparatus (grey arrows). However, the fluorescence of the QDs began to also be co-localized with that of dyes brightening lysosomes from day 3 (white arrows). The efficient intracellular QDs labeling after endocytosis lasted at least 7 days in both cell models, indicating the well-preserved structural integrity of QDs.

3.6. Acute cytotoxic effect of QDs on proliferation-restricted cell cultures

Compared with the non-proliferating HUVEC cells, THP-1 MΦ was more susceptible to the QDs at identical concentrations (Fig. 4A and B). The QDs elicited harmful effect on THP-1 MΦ at 500 nM, with an *IC50* value of 2215 nM. The acute cytotoxic effects of QDs on non-proliferating HUVEC cells were not observed when the concentration of QDs was less than 1000 nM, with an *IC50* value of 3555 nM. The higher QDs-associated acute cytotoxic effect on THP-1 MΦ cells may be the consequence of the higher cellular uptake levels of QDs, which is in line with previous studies [23]. Moreover, QDs at 100 nM significantly increased the production of IL-6 in THP-1 MΦ cells, suggesting the elevation of proinflammatory response (evoked by QDs) prior to the observation of significant acute cytotoxicity (Fig. 4C). Excessive intracellular oxidative stress is another deleterious effect caused by nanoparticles that compromise cell function and survival. Hence, we evaluated the roles of 6-arm PEG-amine/mPEG QDs on excessive intracellular oxidative stress and its secondary effects, such as mitochondrial damage, by performing intracellular ROS level, MMP and LMP assay [34]. These tests were firstly performed in acute cytotoxicity studies, where both cell models generated significantly higher intracellular ROS after exposed to the 250 nM QDs for 24 h (Fig. 4D and E). Similarly, mitochondria with a higher level of damage were noted at the same QDs concentration (Fig. 4F and G). Notably, the 6-arm PEG-amine/mPEG QDs exacerbated lysosomal membrane damage at 100 nM, which is lower than the concentrations triggering measurable intracellular ROS and MMP decrease (Fig. 4H and I).

3.7. Sub-acute cytotoxic effect of QDs on proliferation-restricted cell cultures

In order to explore the longer time impact of intracellular QDs on cells, THP-1 MΦ cells and non-proliferating HUVEC cells were incubated with the 6-arm PEG-amine/mPEG QDs in the proliferation-restricted condition for 24 h and subsequently kept culturing in

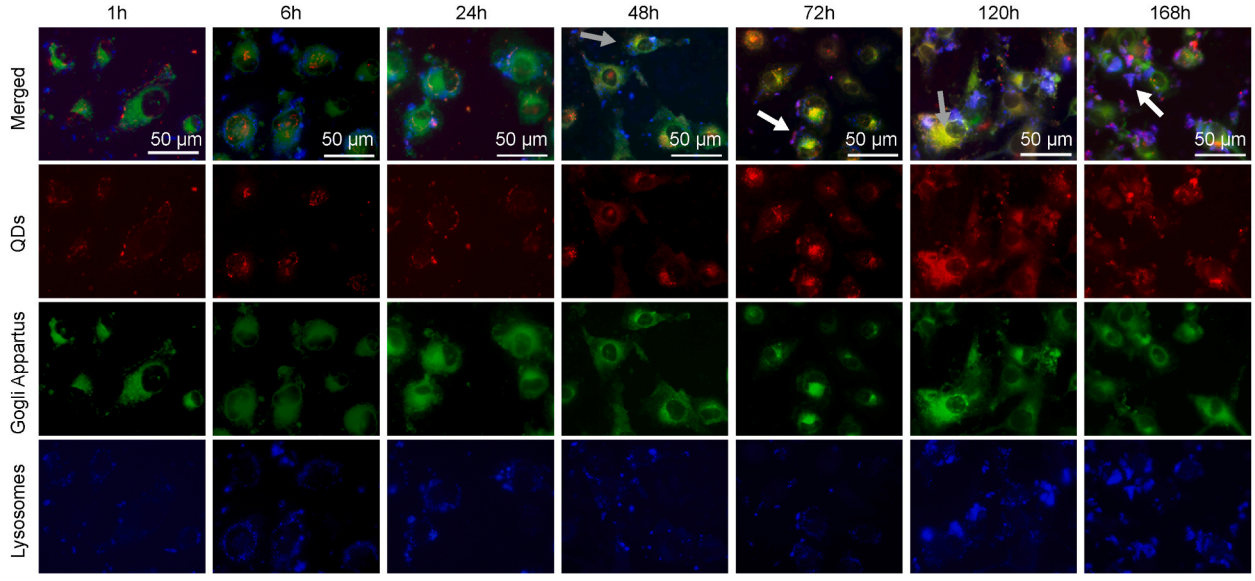

Fig. 3. Representative fluorescence images of spatiotemporal intracellular distribution of 6-arm PEG-amine/mPEG QDs in non-proliferating HUVEC cells. Non-proliferating HUVEC cells were exposed to QDs (500 nM) for 6 h, then the QDs were removed, and cells were kept cultured for different time points (1, 6, 24, 48, 72, 120 and 168 h). Once above given time points achieved, cells loaded with QDs (red) were stained with fluorescent dye labeling Golgi apparatus (green) and lysosome (blue) for 30 min, respectively, and were imaged under fluorescent microscope. Intracellular QDs were mainly transferred to Golgi apparatus initially (merged images, grey arrows), and colocalization of QDs and lysosomes were significantly increased after 72 h (merged images, white images).

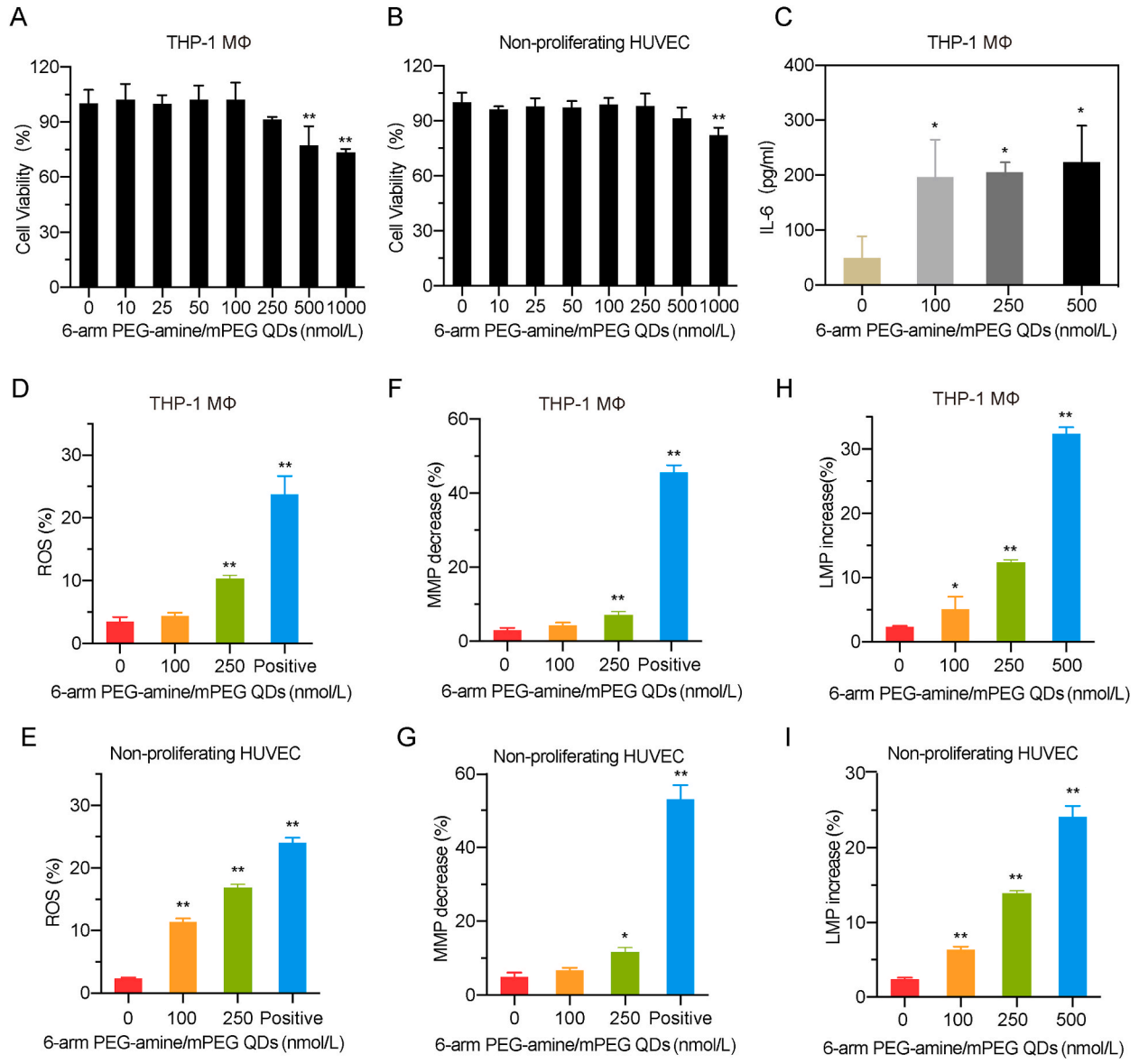

Fig. 4. Acute cytotoxicity of 6-arm PEG-amine/mPEG QDs. (A and B) Cell viabilities of THP-1 MΦ cells and non-proliferating HUVEC cells after exposure to QDs at different concentrations for 24 h, which were expressed as percentage related to the untreated control cells, showing an acute cytotoxic effect on THP-1 MΦ cells at 500 nM and non-proliferating HUVEC cells at 1000 nM. **(C)** Levels of IL-6 produced by THP-1 MΦ cells after QDs incubation for 24 h at different concentrations were detected using ELISA. Release of IL-6 were significantly elevated when QDs concentration higher than 100 nM, indicating the acute proinflammatory effects of 6-arm PEG-amine/mPEG QDs on THP-1 MΦ cells. **(D–I)** Levels of ROS, MMP and LMP in THP-1 MΦ cells and non-proliferating HUVEC cells exposed to QDs at different concentrations for 24 h are subsequently determined using flow cytometry. Normal medium without QDs (0 nM) was used as negative control for all assays. Rosup and CCCP, which provided by manufacturer, was used as the positive control for ROS and MMP, respectively. Significant increase of ROS was found at 250 nM (THP-1 MΦ cells) and 100 nM (non-proliferating HUVEC cells). Significant deterioration of MMP was found at 250 nM in both cell models. In addition, significant enhance of LMP was found at 100 nM in both cell models, implying that it was more sensitive than ROS and MMP detection.

the proliferation-restricted condition for one week, which was referred to as the sub-acute cytotoxicity test. In previous studies, the concentration of QDs that was innocuous in acute cytotoxicity tests were further used for sub-acute cytotoxicity tests [23,28]. In our study, the *IC5* value of each cell model, 78 nM for THP-1 MΦ cells and 140 nM for non-proliferating HUVEC cells, were used for sub-acute cytotoxicity assay. After incubation with QDs for 24 h, no significant adverse effect on viability of both cell models was noted within the first 5 days (Fig. 5A and B). However, the cytotoxic effects were found to increase with time between 5 and 7 days. This, coupled with the significant reduction of cell viability on day 7 (approximately 70% for THP-1 MΦ and 60% for non-proliferating HUVEC cells), implying that the QDs concentration not evoking any acute cytotoxicity could still lead to deleterious effects on cells

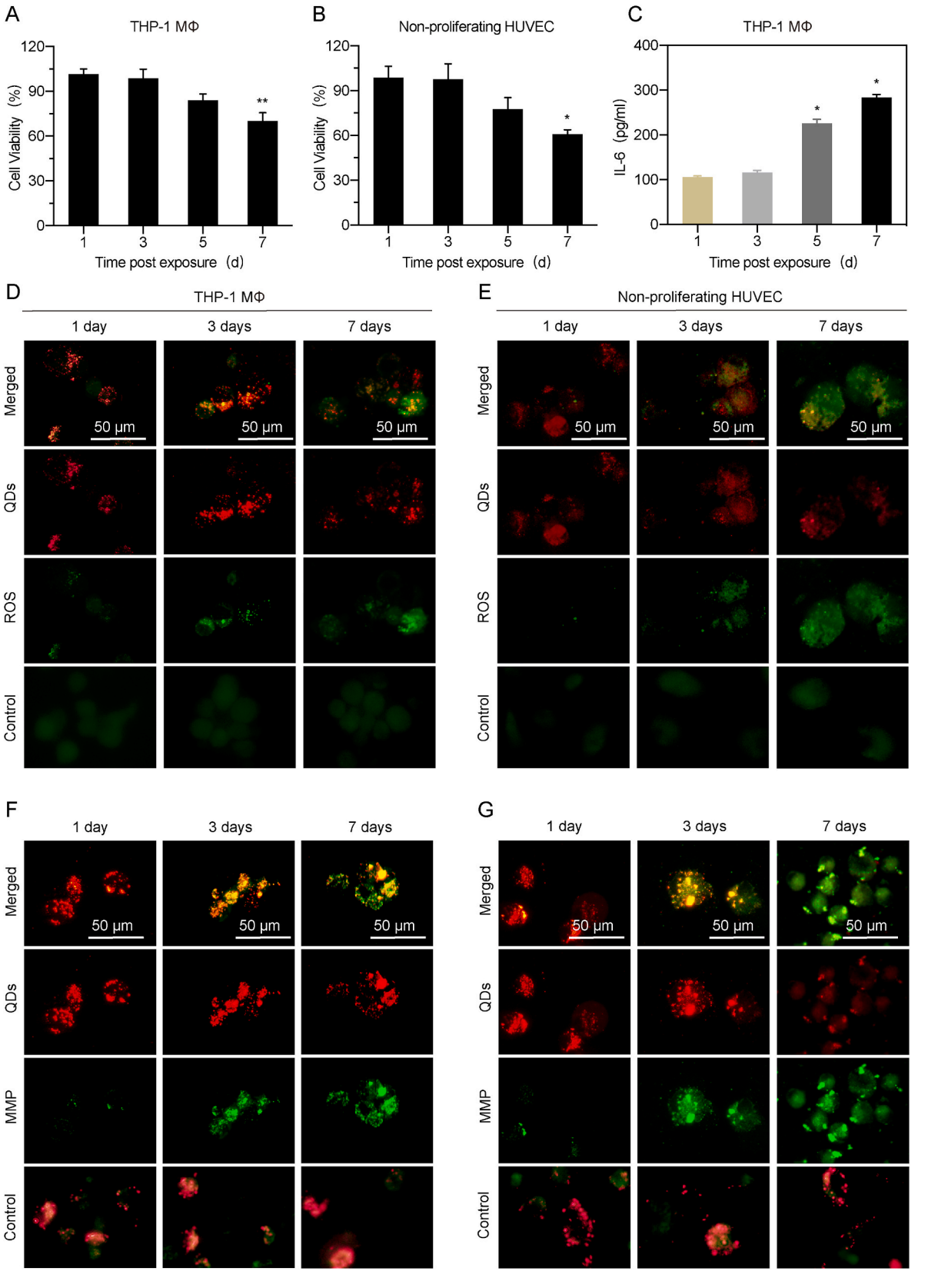

(caption on next page)

Fig. 5. Sub-acute cytotoxicity of 6-arm PEG-amine/mPEG QDs (A and B) THP-1 MΦ cells and non-proliferating HUVEC cells were incubated with QDs for 24 h at *IC5* values determined by acute cytotoxic assays, then unbounded QDs were removed, and cells were cultured in the next 7 days. Cell viabilities were detected using alamar blue assay. The results showed a sub-acute cytotoxic effect on both of cells after 7 days, which were expressed as percentage related to the cells 1-day post exposure. **(C)** Levels of IL-6 produced by THP-1 MΦ cells during this time period were detected using ELISA. Release of IL-6 were significantly elevated on the day 5, earlier than decrease of cell viability. **(D–G)** Levels of ROS and MMP in THP-1 MΦ cells and non-proliferating HUVEC cells under the identical sub-acute cytotoxicity condition are subsequently imaged by microscope. Obviously, increase of ROS and deterioration of MMP were showed after 3 days. Cell models maintained in the normal medium without QDs were used as negative control group. For ROS of both groups, red fluorescence was emitted by intracellular QDs, and the level of ROS was observed by enhancement of green fluorescence. For MMP of experimental group, red fluorescence was emitted by intracellular QDs, and loss of MMP was observed by enhancement of green fluorescence. For MMP of control group, red fluorescence indicated the normal MMP while the green fluorescence showed low MMP. The same green fluorescence and red/green fluorescence ratio at the day 1, day 3 and day 7 demonstrated that the ROS generation and MMP remained unchanged during the whole prolonged cultural period.

after a prolonged period. Interestingly, the viability of non-proliferating HUVEC cells was lower than THP-1 MΦ cells at respective *IC5*. This is in contrast with the result of acute cytotoxicity assays. The proinflammatory response might be associated with the QDs-induced sub-acute cytoxicity, since IL-6 released by THP-1 MΦ cells were significantly higher after day 5 (Fig. 5C).

3.8. Oxidative stress induced sub-acute toxic effects by QDs at a concentration showing negligible acute cytotoxicity

The intracellular ROS and MMP of each proliferation-inhibited cell model at 1, 3, 5 and 7 days following 24 h incubation with 6-arm PEG-amine/mPEG QDs at corresponding IC5 concentration were evaluated. As shown in Fig. 5D, the intracellular ROS level of THP-1 MΦ cells exhibited a time-dependent increase, beginning at 72 h after QDs exposure (brighter green fluorescence). The ROS level of control cells remained low over the same period of time. From the Fig. 5F, the damaged mitochondria of THP-1 MΦ cells were also observed at the same time, suggesting deleterious secondary effects emerged quickly accompanying the increased ROS, whereas the healthy mitochondria were maintained in the control group after 7 days (high red fluorescence). For non-proliferating HUVEC cells, the intracellular ROS level and damaged mitochondria also increased after 72 h of QDs exposure (green fluorescence in the Fig. 5E and G) and further increased after 7 days. Simultaneously, the control group kept the minimal ROS generation and intact mitochondria.

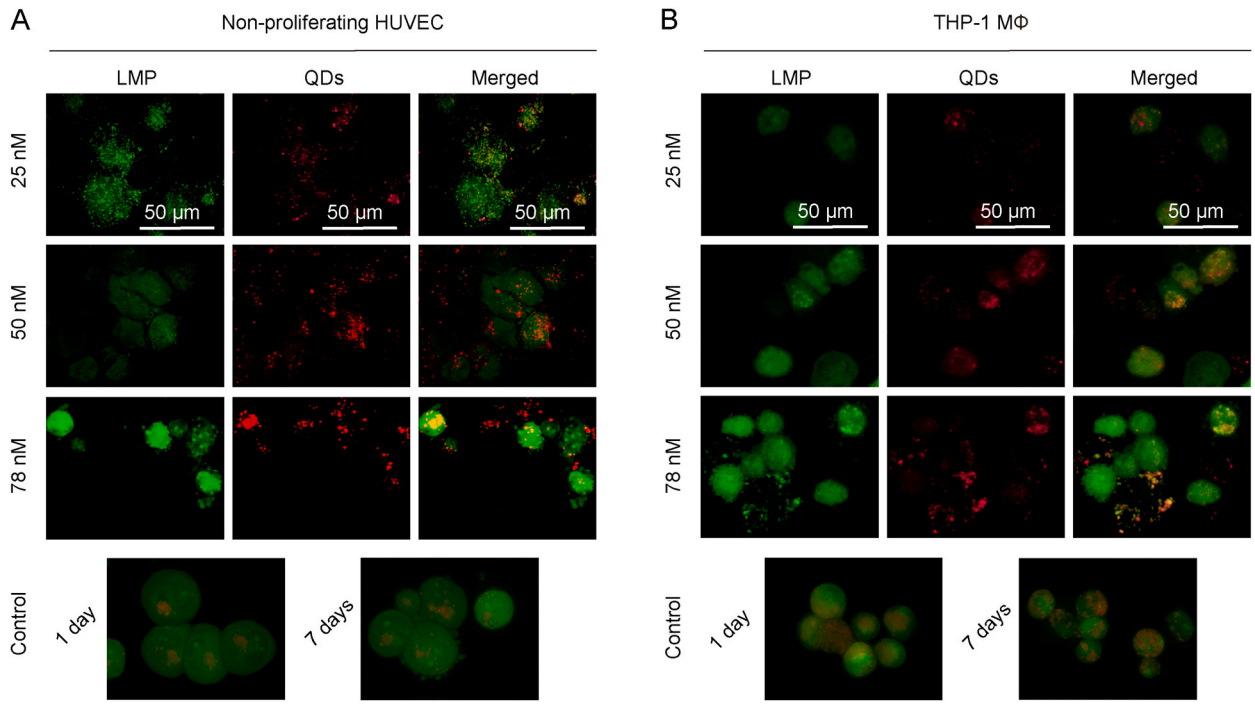

Fig. 6. Non-toxic concentration of 6-arm PEG-amine/mPEG QDs at the sub-acute level THP-1 MΦ cells (A) and non-proliferating HUVEC cells (B) were incubated with QDs for 24 h at 25, 50 and 78 nM, after that, QDs-containing medium were removed, and cells were cultured for 7 days and the LMP were subsequently detected using microscope. The results demonstrated that QDs concentration below 50 nM were supposed to be non-toxic concentration of 6-arm PEG-amine/mPEG QDs at sub-acute cytotoxic levels. Cell models maintained in the normal medium without QDs were used as negative control group. For LMP of experimental group, red fluorescence was emitted by intracellular QDs, and the deterioration of LMP was measured by enhancement of green fluorescence. For LMP of control group, red fluorescence indicated the normal LMP while the green fluorescence showed damaged LMP. The same red/green fluorescence ratio at the day 1 and day 7 showed that the LMP of both cell models were stable during the whole prolonged cultural period.

Two cell cultures showed the consistent response. The excessive intracellular ROS generation and damaged mitochondria were both observed at day 3, earlier than the significant decrease of cell viability observed at day 7. These results highlight the inadequacy of acute cytotoxicity assay to assess the safety impact of QDs. Additionally, membrane damage detections appear to be more sensitive than cell viability assays, such as MTT and CCK8, emphasizing their important role in the early identification of cell injury.

3.9. Determination of non-toxic concentrations of 6-arm PEG-amine/mPEG QDs at the sub-acute cytotoxic levels

In order to identify the concentration of 6-arm PEG-amine/mPEG QDs avoid of sub-acute cytotoxicity, LMP assay were performed in this study due to its high sensitivity. Following incubation with QDs at the concentration of 25, 50 and 78 nM (*IC5* value of THP-1 MΦ cells) for 24 h, the two cell models were maintained in medium with proliferation-restricted condition and the LMP were assessed after 7 days. No significant changes of LMP in cell models were found in the next 7 days post exposure to ≤50 nM QDs (Fig. 6 and Figure S5). Therefore, 50 nM may be defined as the non-toxic concentration of 6-arm PEG-amine/mPEG QDs at the sub-acute cytotoxicity level, which is considerably lower than that in acute cytotoxicity assay, i.e., 250 nM by cell viability assay and 100 nM by LMP assay. Nonetheless, 50 nM is far higher than that commonly used in live cell labeling (1–10 nM) [35], suggesting the possibility of safe clinic applications of 6-arm PEG-amine/mPEG QDs. Although the longer-term fate of cells and intracellular QDs needed to be further elucidated, our data have shown that a panel of tests focusing on membrane damages using adoptable proliferation-restricted cell models at sub-acute toxic level is a highly valuable approach in the biosafety assessment of nanomaterials.

4. Discussion

Near-infrared fluorescent QDs exhibited a great potential in *in vivo* biomedical applications, among which the branched PEG-amine/mPEG QDs showed particular advantages. However, possible biosafety issues surrounding branched PEG-amine/mPEG QDs must be ruled out before clinical translation of this nanomaterial. Previous studies suggested that this type of QDs exhibit a long half-life in blood and showed no obvious *in vivo* toxicity after treatment for 2 months. After intravenous injection, QDs were mainly accumulated in the liver and spleen. Then most of QDs were cleared though fecal excretion and do not have harmful effect on each organ observed by histology analysis [16,18,20]. However, the current cytotoxicity evaluation regarding branched PEG-amine/mPEG QDs is limited to the acute level using inappropriate cancer cell lines. Thus, its cytotoxicity over a prolonged co-incubation period with cells in the blood is unknown till now. The present study more thoroughly evaluated the toxicity of branched PEG-amine/mPEG QDs via systematic investigation of the cellular uptake, intracellular behavior, and related acute and sub-acute cytoxicity under conditions mimicking *in vivo* biomedical applications via intravenous injection.

To assess the cytotoxicity of branched PEG-amine/mPEG QDs, the first step is to prepare corresponding QDs and to establish a reliable *in vitro* cell model that closely mimics the *in vivo* environment. Considering that near-infrared QDs cannot be detected using currently existing fluorescent microscope, we replaced them with the classical ZnCdSe/ZnS core-shell QDs with visible light emission spectra, which has similar size and morphology, as the core and modified them with the branched PEG-amine/mPEG for more convenient and reliable measurement and evaluation. It should be noted that ZnCdSe/ZnS core-shell QDs was only used as the model to explore the cellular uptake and intracellular distribution. This approach may be adopted to study other QDs systems since it was found to be effective in our study. Secondly, to investigate sub-acute toxic effects of QDs on the cells representative of the circulatory system, the use of relative cancer cell lines or long-lived cell lines is inappropriate, despite they are highly reproducible, inexpensive and easy to cultivate. This is because they may exhibit masked cytotoxicity owing to the dilution of the intracellular QDs' contents by rapid cell division [30]. We overcome this problem by establishing non-proliferating cell models of HUVEC and THP-1 cell lines, which can survive for weeks with no proliferating ability [33]. This is a key for successful study of sub-acute level cytotoxicity in this work.

The non-specific binding of QDs depends on the degree of interaction between QDs and cell membranes, which precedes cellular internalization. Stronger QD-cells interactions lead to more cellular internalization of QDs, eliciting more toxic effects. Such interactions depend on surface charge and chemistry of QDs as well as cell types [12]. Surface PEG-modification could diminish cytotoxic response by significantly decreasing the QD-cells interactions. Furthermore, it was found that PEG with larger molecular weights, longer or branched chains positively correlates with the ability to resist cellular uptake [14]. Accordingly, 6- or 8- arm PEG with high molecular weight were selected in this work. It was suggested that QDs with a cationic surface charge tend to interact more strongly with negatively charged cell membranes, thus having more chances to be taken up by cells. On the contrary, QDs with zwitterionic or slightly negative surface charges interact with cell membranes weaklier, resulting in less cellular uptake [32]. Since the surface charge of PEG-modified QDs were mainly determined by functional groups at the end of PEG chain, the non-specific binding and internalization of QDs could be modulated by tuning terminal groups. Therefore, we successfully neutralized the negative carboxyl terminal tail on the OPA-QDs by positive amino terminal tail of PEG and used the PEG with terminal methoxy groups to further enhance the inhibitory effect, as demonstrated previously [33,52,53]. Compared to linear chain PEG-amine modified QDs at the identical concentrations, the cellular uptake amount of 6-arm PEG-amine/mPEG QDs was reduced by nearly tenfold. Among the cells in the circulatory system, phagocytotic cells, such as monocyte-macrophages, were reported to internalize far more QDs than other cells including erythrocyte and endothelium cells [22]. This was confirmed by our study, where the amount of QDs taken up by THP-1 MΦ cells is about twice that by non-proliferating HUVEC cells after incubation with QDs at the same concentration. In addition, we also showed time-and dose-dependence of cellular uptake of QDs, which is in agreement with previous studies using hepatoma cell lines or nerve-derived cells [23,31].

The cytotoxicity of QDs depends on intracellular events, such as the subcellular trafficking, distribution and elimination of QDs, which are mediated by endocytic pathways. Cells can uptake QDs via micropinocytosis, which includes several endocytic pathways.

The entry of QDs mainly via clathrin-mediated endocytosis brings QDs into endosomes and eventually to lysosomes for degradation (Table 1). QDs may suffer from erosion in the acidic lysosomal environment, losing fluorescence and releasing toxic ions like Cd^{2+} and Pb^{2+} [54]. However, lipid raft-mediated endocytosis traffics QDs by cavesome and into organelles like Golgi apparatus or endoplasmic reticulum, all having a neutral pH. Thus, QDs can be stabilized for a longer period and can more likely be eliminated by exocytosis, resulting much lower cytotoxicity. It was observed that more lipid raft-mediated endocytosis of QDs could be obtained when lipophilic groups were introduced on the QDs with zwitterionic or slightly anionic surface charge [12,32]. In the present study, although both type of endocytic pathways take part in the cellular internalization of 6-arm PEG-amine/mPEG QDs, the results of subcellular

Table 1
Results of endocytic pathway, intracellular localization and acute cytotoxicity in this study and previous studies using the same cells or similar core of QDs with different PEG surface modifications.

Core/ Shell	Modification	Cell identification	Endocytic pathway	Subcellular localization	Exposure time (h)	Toxic Conc. (nM)	Highest Conc. (nM)	Ref.
ZnCdSe/ ZnS△	6-arm PEG-amine/mPEG	HUVEC	Clathrin/lipid raft	Golgi Apparatus/ Lysosome	24	1000	1000	this study
		THP-1 MΦ		Golgi Apparatus		500	1000	
CdSe/ ZnS△	Linear PEG-amine	EJ human bladder cancer cell line	/	Cytoplasm	24	40	80	[36]
CdSe/ ZnS△	Linear PEG-amine	HepG2 cells	/	Lysosome	24	>100	100	[31]
CdSe/ ZnS△	Streptavidin-carboxyl-PEG	MEAR Mouse liver hepatoma cell line	/	/	1	>40	40	[37]
(CdTe/ Se)/ ZnS	Methoxy-PEG	Fetal lung fibroblast/ colon epithelial cells	Clathrin	Lysosome	24	>50	50	[38]
CdSe/ ZnS△	Linear PEG-amine	SK-BR-3 cells	/	/	48	256	256	[39]
CdSe/ ZnS△	PMA	U87 glioma cell lines/ HUVEC	/	No fluorescence at 10 nM for 4 h	72	>100	100	[40]
(CdTe/ Se)/ ZnS	PEG		/	Endosome	24	>20	20	[23]
CdSe/ZnS	PMA	HUVEC	/	Endosome	24	20	30	[27]
CdSe/ZnS	PEG	BCECs/astrocytes/C6 glioma		No fluorescence at 2 nM for 4 h	96	>20	20	[41]
CdSe/ZnS	Hydroxyl-PEG-DHLA	THP-1	/	/	24	200[a]	200	[35]
	Methoxy-PEG-DHLA		/	/		>200	200	
CdSe/ZnS	Wates-soluble	Rat Kidney Cells	/	/		20	160	[42]
CdSe/ZnS	PEG-amine	Hela cells	Clathrin, lipid-raft	lysosome				[32]
	SO_3^--PEG-amine		Clathrin, lipid-raft	Lysosome, Golgi apparatus				
	Phenylalanine-PEG-amine		Lipid-raft (dominant)	Golgi apparatus				
	SO_3^--PEG-amine, oleyl		Lipid-raft (dominant)	Golgi apparatus				
(CdTe/ Se)/ ZnS	PEG-amine	Murine macrophage-like cells	/	Lysosome/ mitochondria	24	>80	80	[43–45]
					48	80		
CdSe/ZnS	PEG	Macrophage cell line RAW264.7; breast cancer cell lines	Clathrin-(dominant) and several pathways	Cytoplasm/ endosome/ Lysosome/lipid droplets	24	>40	40	[46]
CdSe	PEG	NIH 3T3 cell line	/	/	72	>100	100	[47]
CdSe/ZnS	Carboxyl-(no PEG)	Macrophage cell line RAW264.7	/	/	24	1.25	2.5	[48]
CdSe	Aldehyde-PEG	HepG2; NIH 3T3	Clathrin	lysosome	24	50–100	100	[49]
	Aldehyde-PEG oleylamide			Cell membrane, lysosome		10	100	
CdSe/ZnS	Bicelles	Hek293t and Hela	/	Cytoplasm, mitochondria and nucleus	72	<7000	7000	[50]
CdTe	MPA-capped	HepG2 and L02	/	/	24	$<25*10^3$	$100*10^3$	[51]

△: the QDs manufactured by Wuhan Jiayuan. a: *IC50* value is 400 nM. Abbreviations: Conc.: Concentration; PMA: polyisobutylene-alt-maleic anhydride-dodecylamine; DHLA: dihydrolipoic acid; BCECs: Brain capillary endothelial cells.

co-localization imaging revealed that the QDs mostly remained in Golgi apparatus for at least several days, where the bright fluorescence of QDs could be observed after 7 days. Thus, it is suitable for live-cell labeling. Overall, superiority of 6-arm PEG-amine/mPEG QDs are attributed to the cumulative effects of amphiphilic modification, weak anionic charge and appropriate surface lipophilicity. Of course, the preferable endocytic pathways also depend on cell types. For the cells in the circulatory system, phagocytes were reported to also internalize nanomaterials via phagocytosis, whereas red blood cells uptake them merely through passive diffusion [55]. Our results showed that blocking either clathrin-mediated or lipid-raft-mediated pathways cannot completely inhibit the endocytosis of two cell models. Approximately 70% of QDs were hindered by inhibitors in non-proliferating HUVEC cells, suggesting dominance of the micropinocytosis process. However, a lower inhibition about 30% were observed with THP-1 MΦ cells as macrophages, implying the involvement of other pathways in cellular uptake of QDs, e.g., caveolae-mediated pathways or scavenger receptor-dependent pathways. These pathways seem to also preserve the QDs rather than digesting rapidly, but further investigation is needed to firmly establish it.

The significantly decreased cellular uptake and successful lysosomal escape of 6-arm PEG-amine/mPEG QDs suggest it is bio-safe. Our results demonstrated that the acute cytotoxicity of 6-arm PEG-amine/mPEG QDs were remarkably lower than other surface-modified QDs, such as QDs modified with linear PEG-amine (Table 1). Nevertheless, prolonged co-incubation of circulatory system cells with QDs increased the amount of internalized QDs due to the time-dependent cellular uptake and the QDs may be remained inside cells for weeks or longer. This intracellular QDs may exhibit detrimental effects over several days post exposure. Previous studies proved that the sub-acute cytotoxicity of QDs is mainly a result of the release toxic ions and excessive intracellular ROS level [23]. The release of toxic ions from the core of QDs is more readily in the acidic environment of lysosomes. The 6-arm PEG-amine/mPEG QDs successfully evaded entry into lysosome and exhibited structural integrity. Thus, the excessive intracellular ROS should receive more attention. At the acute cytotoxic level, this was evaluated by testing the intracellular ROS generation, proinflammatory cytokine production and related mitochondrial and lysosomal damages after 24 h exposure to QDs. The deleterious acute effects of QDs on ROS

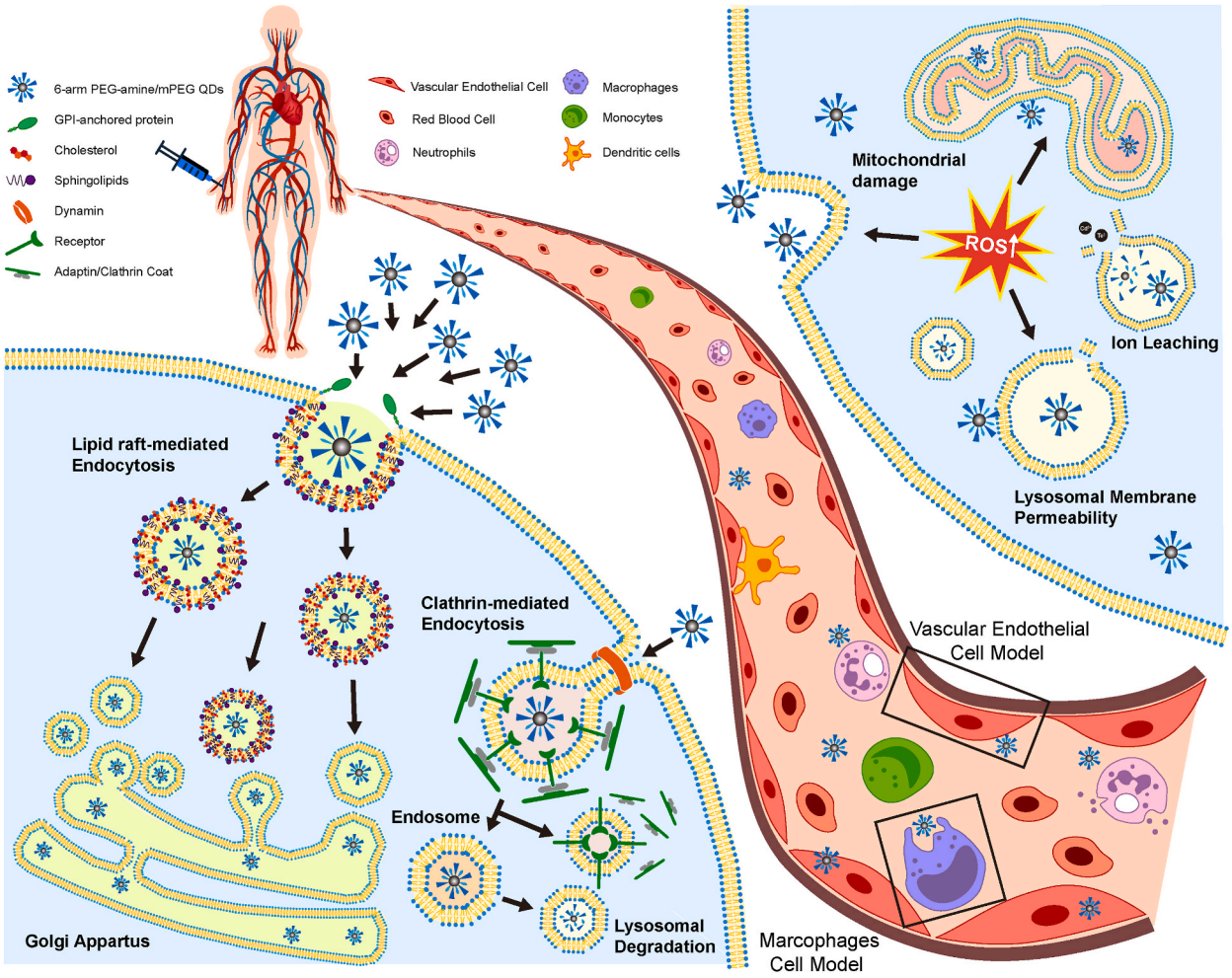

Fig. 7. Schematic illustration for the internalization, subcellular trafficking and localization followed by cytotoxic mechanism of 6-arm PEG-amine/mPEG QDs in the cells in the circulating systems via intravenous administration.

generation were observed at lower concentrations compared with that on cell viability. Intracellular ROS is known to cause the secondary effect and proinflammatory response, which triggers downstream pathways eventually resulting in cell damage and apoptosis. These were usually manifested after several days and may not be observed in acute cytotoxicity tests. Hence, the sub-acute cytotoxicity of 6-arm PEG-amine/mPEG QDs were performed at the concentration presenting non-acute cytotoxic effect (*IC5* value). As expected, significant decrease of cell viability in both cell lines was observed after 5 days post exposure, which coincidences with increased IL-6 production, elevated intracellular ROS level, damaged mitochondria and lysosome. It was clear that concentrations of QDs exerting no acute toxicity can still trigger adverse outcomes at the sub-acute level. Although the sub-acute toxic effect observed in our study was consistent with that reported by Soenen. et al. [23], the mechanisms behind the two studies are different. QDs coated with carboxy, or PEG-amine used by Soenen. et al. were localized in lysosomes and suffered from degradation and leaching of toxic ions, like Cd^{2+}, which led to elevated ROS and interference of metabolic processes. The 6-arm PEG-amine/mPEG QDs exhibited a much lower risk of releasing toxic ions by evading lysosome but still generated ROS by other pathways, such as directly interacting with membrane-bound organelles (Fig. 7). Although we believed that low toxicity of 6-arm PEG-amine/mPEG QDs was closely related to their subcellular localization, it should be proven more directly. For example, the Live/Dead cell dye, Golgi Apparatus dye, Lysosome dye and QDs in one fluorescent image will offer far more sufficient data and ample evidence. However, images like this cannot be provided due to the limitation of fluorescent microscope, which needed to be further improvement. There were several similarities and differences worth noting regarding mechanism of development of acute and sub-acute toxic effects on two cell models. Obviously, the excessive ROS formation played a crucial role both in the acute and sub-acute toxic effects on the THP-1 MΦ cells and non-proliferating HUVEC cells. The ROS formation in the acute toxicity assay occurred immediately after exposure. Fast damage to cell membranes and organelles were also observed at the same time. However, cells in the acute toxicity assay suffered from more negative factors due to the significantly higher QDs concentration. Overdoses resulted in cell surface receptor activation, redox active protein interaction, directly binding with DNA, obstruction of translation machinery. Above processes could all induce toxic effects. In contrast, the redox equilibrium inside cells were broken three days after exposure in the sub-acute toxicity assay followed by membrane and organelles injuries. As shown in the Figs. 2 and 3, during this prolonged incubation time, compared with the highly abundant lysosomes in THP-1 MΦ cells during the whole 7 days, the number of lysosomes in non-proliferation HUVEC cells remarkably increased with time. This difference in the two cell models suggested that the cell homeostasis of HUVEC cells may be perturbed prior to THP-1 MΦ cells. Considering the acidic environment in the lysosome causing the toxic ion leaching from the QDs and acerbating cell dysfunction, it may become one of the mechanisms of sub-acute toxic effects.

QDs exhibited higher sub-acute toxic effects on non-proliferating HUVEC cells than THP-1 MΦ cells after 5- and 7-days post exposure at their respective *IC5* values determined from acute toxicity. This is related to the nearly doubled concentration of QDs incubated with non-proliferating HUVEC cells (140 nM) than with THP-1 MΦ cells (78 nM). Besides, the stability of QDs inside the proliferation-restricted HUVEC cells might be lower, as revealed by the prolonged intracellular imaging analysis. A non-toxic concentration at the sub-acute level for both cell models must be below 78 nM since both types of cell are present in the circulatory system. In fact, we have determined that the maximum non-toxic concentration of 6-arm PEG-amine/mPEG QDs at the sub-acute cytotoxic level is 50 nM, which is almost ten-fold lower than that at the acute cytotoxic level. However, this concentration is still significantly higher than the non-toxic concentration of PEG-amine QDs at the sub-acute cytotoxic level of 20 nM [23], indicating significantly better safety.

It should be noted that the long-term outcome of QDs at non-toxic concentration determined by sub-acute cytotoxic assays remains unknown due to the limitation of proliferation-restricted cell models. The circulatory systems, as a whole, may be resilient after incubation with QDs and leave no sequelae. Nonetheless, non-toxic concentrations of 6-arm PEG-amine/mPEG QDs at the sub-acute toxic level was more than 50 times higher than the concentration that was enough to receive an efficient *in vivo* imaging (<1 nM) [56]. Thus, there is a wide safety margin for promising clinical applications of QDs in terms of diagnosis and treatment. Additionally, the detailed *in vivo* study of branched PEG-amine/mPEG QDs including biodistribution and metabolism needed to be investigated in the future using near-infrared QDs such as Ag-containing QDs.

5. Conclusion

We systematically investigated the cellular internalization, intracellular distribution and cytotoxic effects, at both acute and sub-acute levels, of the QDs modified with branched PEG-amine coupled with mPEG using the proliferation-restricted THP-1 and HUVEC cell models. Consistent with its minimal non-specific binding ability, the cellular uptake of 6-arm PEG-amine/mPEG QDs was nearly ten-fold lower compared with linear PEG-modified QDs. The entry of 6-arm PEG-amine/mPEG QDs into cells through various endocytic pathways and the distribution of intracellular QDs predominantly in Golgi apparatus protected them from degradation for at least one week, which remarkably lowered its acute cytotoxicity. However, QDs at concentrations eliciting no acute cytotoxicity still cause sub-acute cytotoxicity, manifested about 5 days post exposure to QDs, which is associated with the excessive intracellular ROS generation and concomitant membrane damages. Based on the sub-acute toxic evaluation, a preliminary non-toxic concentration of 6-arm PEG-amine/mPEG QDs of 50 nM was identified. This result could offer the safety profile of 6-arm PEG-amine/mPEG QDs and could be an approach for its possible use in a safe way in biomedical applications.

Author contribution statement

Qingyuan Cheng: Conceived and designed the experiments; Performed the experiments; Analyzed and interpreted the data; Wrote the paper.

Yiping Duan: Performed the experiments; Analyzed and interpreted the data.
Wei Fan: Analyzed and interpreted the data; Wrote the paper.
Dongxu Li; Cuiwen Zhu; Tiantian Ma: Performed the experiments.
Jie Liu: Contributed reagents, materials, analysis tools or data.
Mingxia Yu: Conceived and designed the experiments; Contributed reagents, materials, analysis tools or data.

Data availability statement

Data included in article/supplementary material/referenced in article.

Declaration of competing interest

The authors declare that they have no known competing financial interests or personal relationships that could have appeared to influence the work reported in this paper.

Acknowledgments

This work was financially supported by the National Natural Science Foundation of China (Grant No. 81472033 and Grant No. 30901308), Hubei Province Medical Youth Reserve Talents (Young Top Talents) (No. HB20200409), Translational Medicine and Interdisciplinary Research Joint Fund of Zhongnan Hospital of Wuhan University (Grant No. ZNJC202010), Health Commission of Hubei Province Scientific Research Project (Grant No. WJ2019M203) and Zhongnan Hospital of Wuhan University Discipline Seed Fund Project (ZNXKPY2022004). We thank Dr. Zhenya Liu for preparation and characterization of 6-arm PEG-amine/mPEG QDs.

Appendix A. Supplementary data

Supplementary data to this article can be found online at https://doi.org/10.1016/j.heliyon.2023.e20028.

References

[1] A.A.H. Abdellatif, et al., Biomedical applications of quantum dots: overview, challenges, and clinical potential, Int. J. Nanomed. 17 (2022) 1951–1970.
[2] J. Sobhanan, et al., Luminescent quantum dots: synthesis, optical properties, bioimaging and toxicity, Adv. Drug Deliv. Rev. 197 (2023), 114830.
[3] S. Filali, F. Pirot, P. Miossec, Biological applications and toxicity minimization of semiconductor quantum dots, Trends Biotechnol. 38 (2) (2020) 163–177.
[4] Q. Xu, et al., Quantum dots in cell imaging and their safety issues, J. Mater. Chem. B 9 (29) (2021) 5765–5779.
[5] A. Sukhanova, et al., Dependence of quantum dot toxicity in vitro on their size, chemical composition, and surface charge, Nanomaterials 12 (16) (2022).
[6] E. Oh, et al., Meta-analysis of cellular toxicity for cadmium-containing quantum dots, Nat. Nanotechnol. 11 (5) (2016) 479–+.
[7] H. Sun, et al., Cytotoxicity-related bioeffects induced by nanoparticles: the role of surface chemistry, Front. Bioeng. Biotechnol. 7 (2019) 414.
[8] J.C. Zhao, M.H. Stenzel, Entry of nanoparticles into cells: the importance of nanoparticle properties, Polym. Chem. 9 (3) (2018) 259–272.
[9] A. Sukhanova, et al., Dependence of nanoparticle toxicity on their physical and chemical properties, Nanoscale Res. Lett. 13 (2018).
[10] V. Karabanovas, et al., Surface properties of quantum dots define their cellular endocytic routes, mitogenic stimulation and suppression of cell migration, J. Biomed. Nanotechnol. 10 (5) (2014) 775–786.
[11] O. Gladkovskaya, et al., *In* one harness: the interplay of cellular responses and subsequent cell fate after quantum dot uptake, Nanomedicine 11 (19) (2016) 2603–2615.
[12] S. Mazumdar, D. Chitkara, A. Mittal, Exploration and insights into the cellular internalization and intracellular fate of amphiphilic polymeric nanocarriers, Acta Pharm. Sin. B 11 (4) (2021) 903–924.
[13] L. Hu, H. Zhong, Z. He, Toxicity evaluation of cadmium-containing quantum dots: a review of optimizing physicochemical properties to diminish toxicity, Colloids Surf. B Biointerfaces 200 (2021), 111609.
[14] A.S. Karakoti, et al., PEGylated inorganic nanoparticles, Angew Chem. Int. Ed. Engl. 50 (9) (2011) 1980–1994.
[15] T.J. Daou, et al., Effect of poly(ethylene glycol) length on the in vivo behavior of coated quantum dots, Langmuir 25 (5) (2009) 3040–3044.
[16] M.X. Zhang, et al., Bright quantum dots emitting at similar to 1,600 nm in the NIR-IIb window for deep tissue fluorescence imaging, Proc. Natl. Acad. Sci. U. S. A. 115 (26) (2018) 6590–6595.
[17] Z.Y. Liu, et al., Breaking through the size control dilemma of silver chalcogenide quantum dots via trialkylphosphine-induced ripening: leading to Ag2Te emitting from 950 to 2100 nm, J. Am. Chem. Soc. 143 (32) (2021) 12867–12877.
[18] C. Li, et al., Preoperative detection and intraoperative visualization of brain tumors for more precise surgery: a new dual-modality MRI and NIR nanoprobe, Small 11 (35) (2015) 4517–4525.
[19] Z.R. Ma, et al., Near-infrared IIb fluorescence imaging of vascular regeneration with dynamic tissue perfusion measurement and high spatial resolution, Adv. Funct. Mater. 28 (36) (2018) 9.
[20] Y. Zhang, et al., Biodistribution, pharmacokinetics and toxicology of Ag2S near-infrared quantum dots in mice, Biomaterials 34 (14) (2013) 3639–3646.
[21] S. Pandey, A. Mishra, Rational approaches for toxicological assessments of nanobiomaterials, J. Biochem. Mol. Toxicol. 33 (7) (2019) 9.
[22] T. dos Santos, et al., Quantitative assessment of the comparative nanoparticle-uptake efficiency of a range of cell lines, Small 7 (23) (2011) 3341–3349.
[23] S.J. Soenen, et al., The cytotoxic effects of polymer-coated quantum dots and restrictions for live cell applications, Biomaterials 33 (19) (2012) 4882–4888.
[24] P. Urbán, N.J. Liptrott, S. Bremer, Overview of the blood compatibility of nanomedicines: a trend analysis of in vitro and in vivo studies, Wiley Interdiscip Rev Nanomed Nanobiotechnol 11 (3) (2019) e1546.
[25] Z.L. Chen, et al., Preparation of monodisperse hydrophilic quantum dots with amphiphilic polymers, ACS Appl. Mater. Interfaces 9 (46) (2017) 39901–39906.
[26] J.K. Wu, et al., Purification of quantum dot-based bioprobes via high-performance size exclusion chromatography, Talanta 159 (2016) 64–73.
[27] S.J. Soenen, et al., The effect of nanoparticle degradation on poly(methacrylic acid)-coated quantum dot toxicity: the importance of particle functionality assessment in toxicology, Acta Biomater. 10 (2) (2014) 732–741.
[28] B.B. Manshian, et al., High-content imaging and gene expression approaches to unravel the effect of surface functionality on cellular interactions of silver nanoparticles, ACS Nano 9 (10) (2015) 10431–10444.

[29] S. Behzadi, et al., Cellular uptake of nanoparticles: journey inside the cell, Chem. Soc. Rev. 46 (14) (2017) 4218–4244.
[30] F. Joris, et al., Assessing nanoparticle toxicity in cell-based assays: influence of cell culture parameters and optimized models for bridging the in vitro-in vivo gap, Chem. Soc. Rev. 42 (21) (2013) 8339–8359.
[31] L. Peng, et al., Cellular uptake, elimination and toxicity of CdSe/ZnS quantum dots in HepG2 cells, Biomaterials 34 (37) (2013) 9545–9558.
[32] A. Chakraborty, N.R. Jana, Clathrin to lipid raft-endocytosis via controlled surface chemistry and efficient perinuclear targeting of nanoparticle, J. Phys. Chem. Lett. 6 (18) (2015) 3688–3697.
[33] Y.J. Zhang, et al., Functionalized quantum dots induce proinflammatory responses in vitro: the role of terminal functional group-associated endocytic pathways, Nanoscale 5 (13) (2013) 5919–5929.
[34] Y. Wang, M. Tang, Review of in vitro toxicological research of quantum dot and potentially involved mechanisms, Sci. Total Environ. 625 (2018) 940–962.
[35] C.E. Bradburne, et al., Cytotoxicity of quantum dots used for in vitro cellular labeling: role of QD surface ligand, delivery modality, cell type, and direct comparison to organic fluorophores, Bioconjugate Chem. 24 (9) (2013) 1570–1583.
[36] R. Yuan, et al., Effect of quantum dots on the biological behavior of the EJ human bladder urothelial carcinoma cell line, Mol. Med. Rep. 12 (4) (2015) 6157–6163.
[37] J. Zhang, et al., Fluorescent quantum dot-labeled aptamer bioprobes specifically targeting mouse liver cancer cells, Talanta 81 (1–2) (2010) 505–509.
[38] P. Foroozandeh, A.A. Aziz, M. Mahmoudi, Effect of cell age on uptake and toxicity of nanoparticles: the overlooked factor at the nanobio interface, ACS Appl. Mater. Interfaces 11 (43) (2019) 39672–39687.
[39] F. Yao, et al., Purified fluorescent nanohybrids based on quantum dot-HER2-antibody for breast tumor target imaging, Talanta 260 (2023), 124560.
[40] J. Tang, et al., Aptamer-conjugated PEGylated quantum dots targeting epidermal growth factor receptor variant III for fluorescence imaging of glioma, Int. J. Nanomed. 12 (2017) 3899–3911.
[41] N. Huang, et al., Efficacy of NGR peptide-modified PEGylated quantum dots for crossing the blood-brain barrier and targeted fluorescence imaging of glioma and tumor vasculature, Nanomed. Nanotechnol. Biol. Med. 13 (1) (2017) 83–93.
[42] X. Li, H. Zhang, F. Sun, CdSe/ZnS quantum dots exhibited nephrotoxicity through mediating oxidative damage and inflammatory response, Aging (Albany NY) 13 (8) (2020) 12194–12206.
[43] M.J.D. Clift, et al., The impact of different nanoparticle surface chemistry and size on uptake and toxicity in a murine macrophage cell line, Toxicol. Appl. Pharmacol. 232 (3) (2008) 418–427.
[44] M.J.D. Clift, et al., Quantum dot cytotoxicity in vitro: an investigation into the cytotoxic effects of a series of different surface chemistries and their core/shell materials, Nanotoxicology 5 (4) (2011) 664–674.
[45] M.J.D. Clift, et al., The uptake and intracellular fate of a series of different surface coated quantum dots in vitro, Toxicology 286 (1–3) (2011) 58–68.
[46] Q.Q. Liu, et al., Role of surface charge in determining the biological effects of CdSe/ZnS quantum dots, Int. J. Nanomed. 10 (2015) 7073–7088.
[47] Y. Liu, et al., The influence on cell cycle and cell division by various cadmium-containing quantum dots, Small 9 (14) (2013) 2440–2451.
[48] X.M. Wang, et al., Immunotoxicity assessment of CdSe/ZnS quantum dots in macrophages, lymphocytes and BALB/c mice, J. Nanobiotechnol. 14 (2016) 12.
[49] S.J. Tan, et al., Surface-Ligand-dependent cellular interaction, subcellular localization, and cytotoxicity of polymer-coated quantum dots, Chem. Mater. 22 (7) (2010) 2239–2247.
[50] J.M. Fang, et al., Cellular localization, aggregation, and cytotoxicity of bicelle-quantum dot nanocomposites, ACS Appl. Bio Mater. 6 (2) (2023) 566–577.
[51] T. Zhang, et al., MPA-capped CdTequantum dots induces endoplasmic reticulum stress-mediated autophagy and apoptosis through generation of reactive oxygen species in human liver normal cell and liver tumor cell, Environ. Pollut. 326 (2023), 121397.
[52] M. Ulusoy, et al., Aqueous synthesis of PEGylated quantum dots with increased colloidal stability and reduced cytotoxicity, Bioconjugate Chem. 27 (2) (2016) 414–426.
[53] A.H. Silva, et al., Superparamagnetic iron-oxide nanoparticles mPEG350-and mPEG2000-coated: cell uptake and biocompatibility evaluation, Nanomed. Nanotechnol. Biol. Med. 12 (4) (2016) 909–919.
[54] S.J. Soenen, et al., (Intra)Cellular stability of inorganic nanoparticles: effects on cytotoxicity, particle functionality, and biomedical applications, Chem. Rev. 115 (5) (2015) 2109–2135.
[55] S.J. Soenen, et al., Cellular toxicity of inorganic nanoparticles: common aspects and guidelines for improved nanotoxicity evaluation, Nano Today 6 (5) (2011) 446–465.
[56] C.-N. Zhu, et al., Near-infrared fluorescent Ag2Se-cetuximab nanoprobes for targeted imaging and therapy of cancer, Small 13 (3) (2017).